Applied Meteorology Unit (AMU)

Quarterly Report

Second Quarter FY-01

Contract NAS10-96018

30 April 2001

ENSCO, Inc.
1980 N. Atlantic Ave., Suite 230
Cocoa Beach, FL 32931
(321) 853-8202 (AMU)
(321) 783-9735

Distribution:

NASA HQ/Q/F. Gregory
NASA KSC/AA/R. Bridges
NASA KSC/MK/J. Halsell
NASA KSC/PH/D. King
NASA KSC/PH/E. Mango
NASA KSC/PH/M. Leinbach
NASA KSC/PH/M. Wetmore
NASA KSC/PH-A/J. Guidi
NASA KSC/YA/K. Payne
NASA KSC/YA-C/D. Bartine
NASA KSC/YA-D/H. Delgado
NASA KSC/YA-D/J. Madura
NASA KSC/YA-D/F. Merceret
NASA KSC/YA-C/G. Allen
NASA JSC/DA8/W. Hale
NASA JSC/MA/R. Dittemore
NASA JSC/MS2/C. Boykin
NASA JSC/ZS8/F. Brody
NASA MSFC/ED03/S. Pearson
NASA MSFC/ED44/D. Johnson
NASA MSFC/ED44/B. Roberts
NASA MSFC/ED44/G. Jasper
NASA MSFC/MP01/A. McCool
NASA MSFC/MP71/S. Glover
45 WS/CC/N. Wyse
45 WS/DO/M. Christie
45 WS/DOR/D. Beberwyk
45 WS/DOR/D. McCabe
45 WS/DOR/J. Sardonia
45 WS/DOR/J. Tumbiolo
45 WS/DOR/E. Priselac
45 WS/DOR/J. Weems
45 WS/SY/D. Harms
45 WS/SYR/W. Roeder
45 WS/SYA/B. Boyd
45 OG/CC/D. Mitchell
45 LG/CC/S. Fancher
45 LG/LGP/R. Fore
CSR 7000/M. Maier
CSR 4140/H. Herring
45 SW/SESL/D. Berlinrut
SMC/CWP/M. Coolidge
SMC/CWP/T. Knox
SMC/CWP/R. Bailey
SMC/CWP (PRC)/P. Conant
Hq AFSPC/DORW/S. Carr
Hq AFWA/CC/C. French
Hq AFWA/DNX/E. Bensman
Hq AFWA/DN/N. Feldman
Hq USAF/XOW/H. Tileston
Hq AFRL/XPPR/B. Bauman
Office of the Federal Coordinator for Meteorological Services and Supporting Research

SMC/SDEW/L. Hagerman
NOAA “W/NP”/L. Uccellini
NOAA/OAR/SSMC-I/J. Golden
NOAA/NWS/OST12/SSMC2/J. McQueen
NOAA Office of Military Affairs/L. Freeman
Aerospace Corp/T. Adang
NWS Melbourne/B. Hagemeyer
NWS Southern Region HQ/“W/SRH”/X. W. Proenza
NWS Southern Region HQ/“W/SR3”/D. Smith
NSSL/D. Forsyth
NWS/“W/OSD5”/B. Saffle
FSU Department of Meteorology/P. Ray
NCAR/J. Wilson
NCAR/Y. H. Kuo
30 WS/SY/C. Crosiar
30 WS/CC/P. Boerlage
30 SW/XP/J. Hetrick
NOAA/ERL/FSL/J. McGinley
ENSCO Contracts/E. Lambert

Executive Summary

This report summarizes the Applied Meteorology Unit (AMU) activities for the second quarter of Fiscal Year 2001 (January – March 2001). A detailed project schedule is included in the Appendix.

Ms. Lambert continued work on the Statistical Short-Range Forecast Tools task with the goal of developing short-range ceiling forecast equations to be used in support of Shuttle landings at the Shuttle Landing Facility. She developed and tested 3-hour observations-based and persistence climatology forecast equations. Tests of the 3-hour observations-based equations yielded similar results to the 1- and 2-hour equations in that they showed an improvement over the persistence climatology forecasts. The probability of detection (POD) and false alarm rate (FAR) scores were calculated for all three lead times. In general, POD decreased and FAR increased with increasing lead time, indicating a degradation in performance as lead time increases.

Dr. Manobianco and Mr. Wheeler began work to transition the new Stratified Logistic Thunderstorm Index (SLTI) developed at the Air Force Institute of Technology, which will replace the Neumann-Pfeffer thunderstorm probability index (NPTPI) currently used by the 45th Weather Squadron (45 WS). Initial results with SLTI show improvement over NPTPI, and the 45 WS has requested that the new SLTI be implemented for forecaster use before the 2001 warm season. Dr. Manobianco and Mr. Wheeler developed several Man-computer Interactive Data Access System data decoders to calculate the required input variables, developed data decoders, compiled the SLTI FORTRAN code on an AMU workstation, and benchmarked the SLTI against persistence.

Dr. Short completed Phase II of the SIGMET Interactive Radar Information System Processor Evaluation task and generated a memorandum describing the results. He developed seasonally varying scan strategies based on seasonal temperatures over Cape Canaveral Air Force Station for the Weather Surveillance Radar, model 74C (WSR-74C) located at Patrick Air Force Base. After reviewing the results, 45 WS personnel determined that the present scan strategy provides excellent coverage during both summer and winter and that special scan strategies for the cool and warm seasons are not necessary.

Mr. Wheeler and Mr. Dianic completed software modifications in support of the Airborne Field Mill (ABFM) campaign in February. The ABFM program is designed to improve the lightning launch criteria for Shuttle and expendable launch vehicles. The AMU was tasked to upgrade the software used to superimpose the location of the ABFM research aircraft on WSR-74C radar images. Mr. Wheeler also provided technical support during the field experiment.

Mr. Wheeler and Dr. Short continued work on the MiniSODAR™ evaluation. Boeing plans to install a MiniSODAR™ at the new Space Launch Complex 37 instead of a tall wind tower to evaluate the launch pad winds during ground and launch operations. In order to make critical GO/NO GO launch decisions, forecasters need to know the quality of the data. Therefore, Mr. Wheeler and Dr. Short were tasked to perform an objective comparison between the False Cape MiniSODAR™ wind observations and those from the closest tall wind towers.

Mr. Case completed the evaluation of the Regional Atmospheric Modeling System (RAMS) component of the Eastern Range Dispersion Assessment System (ERDAS). He generated a final report that presents objective and subjective evaluations conducted for the 1999 and 2000 warm seasons, and the 1999-2000 cool season. Mr. Case completed work on Phase III of the Local Data Integration System (LDIS) task, which calls for AMU assistance to install a working LDIS at the Spaceflight Meteorology Group (SMG) and the National Weather Service in Melbourne, FL (NWS MLB). LDIS generates routine high-resolution products for operational guidance. He helped SMG correct a problem in the cloud analysis portion of the LDIS, and worked with NWS MLB to solve their radar data ingest problem.

Mr. Dianic continued work on the extension and enhancement of the ERDAS RAMS Evaluation task to improve the archived database, and to perform sensitivity tests to identify the possible cause(s) of the model cold bias. He prepared a draft memorandum that discusses a proposed data transfer mechanism for sending a subset of real-time RAMS forecasts to SMG and NWS MLB, completed the recovery of RAMS 3-grid forecasts for the 1999-2000 cool season that were lost due to a disk crash, and completed development of scripts to run RAMS sensitivity experiments on the AMU HP workstation.

Table of Contents

Executive Summary iii

SPECIAL NOTICE TO READERS 1

1. BACKGROUND 1

2. AMU ACCOMPLISHMENTS DURING THE PAST QUARTER 1

2.1 TASK 003 SHORT-TERM FORECAST IMPROVEMENT 1

SUBTASK 3 Statistical Short-Range Forecast Tools (Ms. Lambert) 1

SUBTASK 6 Neumann-Pfeffer Index Replacement (Dr. Manobianco and Mr. Wheeler) 3

2.2 TASK 004 INSTRUMENTATION AND MEASUREMENT 3

SUBTASK 12 SIGMET IRIS/OPEN Processor Evaluation (Dr. Short) 3

SUBTASK 12.1 Aircraft position Radar Overlay (Mr. Wheeler and Mr. Dianic) 6

SUBTASK 13 Mini-SODAR Evaluation (Dr. Short and Mr. Wheeler) 6

SUBTASK 5 I&M and RSA Support (Dr. Manobianco, Mr. Case, and Mr. Wheeler) 8

2.3 TASK 005 MESOSCALE MODELING 9

SUBTASK 8 Meso-Model Evaluation (Mr. Case) 9

SUBTASK 10 Local Data Integration System Phase III (Mr. Case) 14

SUBTASK 11 Extension / Enhancement of the ERDAS RAMS Evaluation (Mr. Case and Mr. Dianic) 15

2.4 AMU CHIEF'S TECHNICAL ACTIVITIES (DR. MERCERET) 15

2.5 TASK 001 AMU OPERATIONS 15

List of Acronyms 17

Appendix A 19

SPECIAL NOTICE TO READERS

Applied Meteorology Unit (AMU) Quarterly Reports are temporarily unavailable on the Wide World Web (WWW). Notice of its availability will be posted in this section.

The AMU Quarterly Reports are also available in electronic format via email. If anyone on the current distribution would like to be added to the email list, please send your email address to Winifred Lambert (321-853-8130, lambert.winifred@ensco.com). If any of your mailing information changes or if you would like to be removed from the distribution list, please notify Frank Merceret (321-867-0818, francis.merceret-1@ksc.nasa.gov) or Winifred Lambert (321-853-8130, lambert.winifred@ensco.com).

1. BACKGROUND

The AMU has been in operation since September 1991. Tasking is determined annually with reviews at least semi-annually. The progress being made in each task is discussed in Section 2 with the primary AMU point of contact reflected on each task and/or subtask. A list of acronyms used in this report immediately follows Section 2.

2. AMU ACCOMPLISHMENTS DURING THE PAST QUARTER

2.1 TASK 003 SHORT-TERM FORECAST IMPROVEMENT

SUBTASK 3 STATISTICAL SHORT-RANGE FORECAST TOOLS (MS. LAMBERT)

The forecast cloud ceiling at the Shuttle Landing Facility (SLF) is a critical element in determining whether a GO or NO GO should be issued for a Space Shuttle landing. However, the Spaceflight Meteorology Group (SMG) forecasters have found that ceiling is a difficult parameter to forecast. The goal of this task is to develop short-range ceiling forecast equations to be used in support of Shuttle landings. Ms. Lambert is using a 19-year record (1979–1997) of hourly surface observations from the SLF and several stations in east-central Florida to develop these equations. The equation development is centered on the ceiling thresholds defined by the Shuttle Flight Rules (FRs) and shown in Table 1.

Table 1. List of Flight Rules for ceiling thresholds at the Shuttle Landing Facility (SLF).

Ceiling Threshold	***Flight Rule***
< 5000 ft	Return to Launch Site (RTLS)
< 8000 ft	End of Mission (EOM)
< 10 000 ft	Navigation Aid Degradation

Ms. Lambert developed the 3-hour observations-based (OBS) forecast equations and tested their performance against the associated persistence climatology equations (PCLIMO). The results are similar to those for the 1- and 2-hour forecasts in that the OBS equations produced improved forecasts over those of the PCLIMO equations. The positive values in Table 2 show the magnitude of that improvement. The improvement increases with increasing lead time, as can be seen in the last row of Table 2 that contains the average values for each column. This may be because persistence looses accuracy at longer lead times and the addition of data from other stations may increase the accuracy of the forecast. For all three lead times, the improvement has a tendency to decrease with decreasing cloud ceiling value. This may be an artifact of fewer observations of lower ceiling height values. Also note that the values for the 1-hour forecast of ceilings < 5000 ft at 02Z and 20Z are close to 0, indicating that persistence climatology is almost equal in performance at those times. Overall, however, the positive values indicate that the OBS forecasts will produce a more accurate probability forecast of ceiling category occurrence at all three lead times.

Table 2. Scores comparing the performance of the observations-based equations to that of the persistence climatology equations. A positive number indicates a percent improvement in forecast skill of the observations-based equations over the persistence climatology equations, and a negative number indicates a percent degradation.

Valid Time of Forecast	***< 10 000 ft***			***< 8000 ft***			***< 5000 ft***		
	1-Hour	**2-Hour**	**3-Hour**	**1-Hour**	**2-Hour**	**3-Hour**	**1-Hour**	**2-Hour**	**3-Hour**
00Z	11.7	7.4	15.5	6.2	6.0	16.6	7.3	4.1	12.4
01Z	10.1	9.0	14.7	6.3	5.8	9.2	7.2	4.7	11.4
02Z	6.8	7.8	10.9	1.8	8.4	7.4	0.2	4.2	9.8
03Z	10.6	13.8	13.1	10.5	12.2	11.9	8.1	8.4	7.7
04Z	14.2	17.6	12.6	14.4	17.3	18.0	13.6	12.6	14.7
05Z	16.7	22.2	18.9	11.3	19.7	16.2	6.7	16.0	12.2
06Z	11.0	17.8	27.2	8.7	18.7	24.7	10.5	10.0	28.2
07Z	12.0	13.2	19.1	8.8	7.6	17.0	6.0	9.4	14.8
08Z	4.1	11.3	8.6	5.1	11.3	6.6	8.5	8.5	9.3
09Z	12.3	18.2	16.7	6.8	15.8	15.5	11.7	20.8	18.0
10Z	10.3	15.2	14.2	7.0	9.8	14.5	8.0	9.4	15.1
11Z	16.9	16.3	16.5	16.4	16.3	16.5	16.4	14.5	17.7
12Z	13.8	20.6	11.6	14.9	21.8	17.4	11.9	18.7	17.2
13Z	15.9	19.4	22.7	12.9	19.9	24.7	8.8	21.3	22.4
14Z	12.0	18.8	23.7	10.9	15.6	13.8	12.0	11.7	22.0
15Z	10.9	17.1	15.4	12.7	13.8	13.6	12.7	8.3	11.0
16Z	17.6	19.5	16.5	17.4	15.6	11.7	11.9	13.7	11.4
17Z	8.3	18.3	7.7	9.6	15.4	8.4	7.8	18.4	7.3
18Z	13.5	13.2	9.1	14.0	16.6	12.8	10.6	12.7	8.0
19Z	7.7	15.0	13.5	8.5	13.0	12.8	8.2	16.6	11.5
20Z	9.6	7.8	14.1	4.8	6.8	10.7	-0.6	13.0	11.1
21Z	11.2	16.1	7.6	7.9	9.5	4.8	3.2	3.5	10.3
22Z	13.2	11.5	11.5	10.4	9.9	8.3	9.7	12.7	6.3
23Z	15.0	19.4	15.8	13.4	16.1	13.7	9.5	13.3	12.8
Mean	**11.9**	**15.2**	**14.9**	**10.0**	**13.5**	**13.6**	**8.8**	**11.9**	**13.4**

In order to determine the potential operational performance of the OBS equations, the probability of detection (POD) and false alarm rate (FAR) scores were calculated using the independent data set. A standard contingency table, as shown in the example below (Wilks 1995), was constructed in order to calculate the POD and FAR scores.

		Observed	
		Yes	No
Forecast	Yes	a	b
	No	c	d

where

$$\text{POD} = \frac{a}{a + c} \quad \text{and} \quad \text{FAR} = \frac{b}{a + b}$$

The observations are categorical and can only have the values 0 for ‘No’ and 1 for ‘Yes’. The forecasts, however, are probabilities and can have values between 0 and 1, inclusive. Ms. Lambert used probabilities ≥ 0.5 as ‘Yes’ forecasts, and those < 0.5 as ‘No’ forecasts. The POD and FAR scores were calculated for the OBS equations, 216 in all (24 hours * 3 lead times * 3 ceiling thresholds). Table 3 shows the 24-hour average values of POD and FAR for the three lead times and three ceiling height thresholds. In Table 2, the improvement over persistence climatology increased with increasing lead time, but Table 3 shows that the actual performance decreases with increasing lead time.

Table 3. The probability of detection (POD) and false alarm rate (FAR) scores of the observations-based equations using the independent data for the three lead times and three ceiling height thresholds.

Forecast Lead Time	***POD***			***FAR***		
	< 10 000 ft	**< 8000 ft**	**< 5000 ft**	**< 10 000 ft**	**< 8000 ft**	**< 5000 ft**
1-Hour	0.83	0.83	0.80	0.16	0.17	0.18
2-Hour	0.73	0.70	0.65	0.21	0.23	0.24
3-Hour	0.67	0.63	0.54	0.25	0.27	0.27

In the next quarter, Ms. Lambert will conduct hypothesis testing to determine the statistical significance of the improvement of the OBS equations over the PCLIMO equations.

References

Wilks, D. S., 1995: *Statistical Methods in the Atmospheric Sciences*. Academic Press, Inc., San Diego, CA, 467pp.

SUBTASK 6 NEUMANN-PFEFFER INDEX REPLACEMENT (DR. MANOBIANCO AND MR. WHEELER)

The Air Force Institute of Technology (AFIT) has developed a Stratified Logistic Thunderstorm Index (SLTI) to replace the Neumann-Pfeffer thunderstorm probability index (NPTPI). Initial results show improvement over NPTPI, and the 45th Weather Squadron (45 WS) has requested that the new SLTI be implemented for forecaster use before the 2001 warm season. This tool will calculate and display the current day’s thunderstorm occurrence probability and display the probable time of occurrence using the NPTPI timing algorithm on the Meteorological Interactive Data Display System (MIDDS). The AMU will demonstrate the NPTPI software capabilities to 45 WS personnel, and all software and tools developed by the AMU will be provided to the 45 WS and assistance, if needed, in the installation of those tools.

In August 2000, Ms. Robin Schumann converted the AFIT SLTI software from Mathcad® to FORTRAN. In February 2001, Mr. Wheeler developed several Man-computer Interactive Data Access System (McIDAS) data decoders to calculate the required input variables. These variables include the six-day persistence pattern of thunderstorms at the SLF, the 800 – 600 mb average relative humidity, the wind direction and speed at 850, 600, and 700 mb, the Thompson Index, and the K Index. Dr Manobianco developed data decoders, compiled the SLTI FORTRAN code on an AMU workstation, and benchmarked the SLTI against persistence using archived surface and rawinsonde data from the 1996 warm season.

2.2 TASK 004 INSTRUMENTATION AND MEASUREMENT

SUBTASK 12 SIGMET IRIS/OPEN PROCESSOR EVALUATION (DR. SHORT)

Phase II of the SIGMET IRIS/OPEN Processor Evaluation task called for the AMU to develop new radar products to enhance the operational capabilities of the 45 WS and SMG. The Interactive Radar Information System (IRIS) provides display and analysis of radar reflectivity data from the Weather Surveillance Radar, model 74C (WSR-74C) located at Patrick Air Force Base. Operational use of the radar and radar products includes evaluation of Launch Commit Criteria (LCC) and FRs, and forecasting for ground operations.

The task was re-scoped in December 2000 to: 1) cease development of new radar products due to technical difficulties, 2) provide detailed information on the new radar products for development of a Request for Quotation (RFQ) to a software vendor and, 3) develop seasonally varying scan strategies based on the seasonal cycle of atmospheric temperatures over Cape Canaveral Air Force Station (CCAFS). An AMU memorandum detailing the technical difficulties, the RFQ information, and the seasonal scan strategies has been generated and distributed to the 45 WS, SMG and the National Weather Service Office in Melbourne, FL (NWS MLB). The following paragraphs give a brief summary of results presented in the memorandum, excluding the RFQ information.

IRIS Capabilities

IRIS provides a broad array of radar products and product displays to assist forecasters in detailed analyses of convectively generated clouds that can threaten both ground and space launch operations with lightning and strong winds. The vertical structure of developing storms is closely monitored, especially when they are within 60 nm of the Kennedy Space Center (KSC)/CCAFS complex and their vertical development penetrates the altitude range of the 0°C to -20°C isotherms, typically between 10 000 and 28 000 ft. Cloud electrification processes are active within this temperature range and local forecasters at CCAFS have developed a number of specialized radar observational techniques for short-term forecasting of lightning and damaging winds. Forecast operations could benefit from development additional radar products that are customized to facilitate implementation of specialized techniques.

IRIS includes a programming feature called the User Product Insert (UPI) for the development of new radar products. It was envisioned that some of the specialized CCAFS radar observational techniques could be enhanced and automated by use of the UPI capability. A list of specialized radar products was developed during Phase I of the task, customized with respect to the operational environment at KSC/CCAFS. Technical difficulties related to proprietary computer code, impacts on system performance, and inadequate documentation were encountered during the development of the new products, resulting in a decision to halt the development effort. As a result, the 45 WS is planning an IRIS User's Workshop (IUW) at the American Meteorological Society's annual meeting in Orlando in January 2002. This IUW has three main goals: 1) establish new products desired by many customers that SIGMET could develop; 2) cross-feed locally developed tools among the customers, and 3) provide feedback to SIGMET on problems needing correction.

Seasonal Scan Strategies

The re-scoped task called for the development of seasonally-varying volume scan strategies and a quantitative evaluation of their impact on the vertical resolution of the radar data. Guidance for the scan strategies was obtained from an analysis of the seasonal cycle of atmospheric temperatures over CCAFS. Temperature climatology data were obtained from the Range Reference Atmosphere, built by the Range Commanders' Council Meteorology Group.

The present scan strategy for the WSR-74C radar, designed by the AMU and implemented in June 2000, has the highest elevation angle reaching the highest expected altitude of the -20°C isotherm over the KSC/CCAFS complex. This assures effective monitoring of the electrically active zone of thunderstorms under the most extreme conditions. A statistical analysis of the temperature climatology data indicates that during the cool season the critical altitude of the -20°C isotherm is about 2000 feet lower than during the warm season. A lowering of the highest radar elevation angle during the cool season would improve the vertical resolution of the radar data and could improve its value for making short-term forecasts of lightning and damaging winds.

The AMU developed a generalized method to automatically calculate a radar scan strategy in order to make recommendations for seasonally-varying scan strategies based on climatological variations in the height of the -20°C isotherm. The method requires the minimum range and maximum altitude to be viewed by the maximum elevation angle, the radar beam width, the number of elevation angles, and the minimum elevation angle. Scan strategies were designed so that the vertical gaps between half-power points of the radar beam were constant with range at a given altitude. The vertical gaps depend on the range of elevation angles and the number of elevation angles in the scan.

Table 4 lists elevation angles of seasonally adjusted scan strategies for the cool and warm seasons in addition to the transition months of April and October. The number of elevation angles was fixed at 12, as in the present configuration, to maintain the 2.5-minute radar update cycle. The minimum elevation angle was set at 0.4° to provide coverage at low altitudes where convective clouds originate. The maximum elevation angle was set to intersect the critical altitude at a ground range of 9.3 nm. This constraint ensures coverage up to the critical altitude over the southern boundary of the KSC/CCAFS area and Space Launch Complex (SLC) 17. The critical altitude was determined by adding two standard deviations (+ 2σ) to the mean height of the -20°C isotherm. The vertical gap was determined at a reference altitude of 18 060 ft, close to the mean annual altitude of the -10°C isotherm. The elevation angle sequences are not dependent on the reference altitude. The values in Table 4 indicate that there is a seasonal-cycle in the vertical gaps for scan strategies that are seasonally adjusted. For example, the vertical gap for the cool season is 6.4 % less than the gap for the warm season. However, this is much less than the 37% reduction achieved when the current scan strategy was adopted under Phase I of the task.

Table 4. Elevation angles for seasonal scan strategies. The critical altitude corresponds to the +2σ level of the -20ºC isotherm for the month or season.

Elevation Angle (°)	***Cool Season***	***April Transition***	***Warm Season***	***October Transition***
$\boldsymbol{\theta_{12}}$	24.70	25.00	26.00	25.40
$\boldsymbol{\theta_{11}}$	21.32	21.56	22.36	21.88
$\boldsymbol{\theta_{10}}$	18.20	18.39	19.01	18.64
$\boldsymbol{\theta_{9}}$	15.35	15.49	15.96	15.68
$\boldsymbol{\theta_{8}}$	12.75	12.85	13.20	12.99
$\boldsymbol{\theta_{7}}$	10.40	10.47	10.72	10.57
$\boldsymbol{\theta_{6}}$	8.27	8.32	8.49	8.39
$\boldsymbol{\theta_{5}}$	6.36	6.39	6.50	6.43
$\boldsymbol{\theta_{4}}$	4.64	4.66	4.72	4.68
$\boldsymbol{\theta_{3}}$	3.09	3.09	3.12	3.11
$\boldsymbol{\theta_{2}}$	1.68	1.69	1.70	1.69
$\boldsymbol{\theta_{1}}$	0.40	0.40	0.40	0.40
Vertical Gap at 18 060 ft (ft)	1891	1921	2020	1962
Critical Altitude (ft)	25 700	26 100	27 200	26 600

On 26 January 2001 Dr. Short met with Mr. Roeder and Mr. Pinder of the 45 WS to discuss the vertical resolution of scan strategies shown in Table 4. After reviewing the results, they determined that the present scan strategy provides excellent coverage of the electrically active region of clouds up to the -20ºC isotherm level during both summer and winter and that a special scan strategy for the cool season is not necessary. Since the current scan strategy was optimized for year-round 0°C to -20°C heights and height variability, it already accounts for the highest -20°C heights during the summer. Because the current scan strategy is practically indistinguishable from the warm season scan strategy, the results of this section indicate that the current scan strategy can be used throughout the year.

SUBTASK 12.1 AIRCRAFT POSITION RADAR OVERLAY (MR. WHEELER AND MR. DIANIC)

The aircraft position radar overlay task is funded by KSC under AMU option hours. The AMU was tasked to superimpose the location of the research aircraft from the Airborne Field Mill (ABFM) experiment on WSR-74C SIGMET radar images. The ABFM experiment collects data to allow safe revision of the lightning launch commit criteria to provide greater launch availability. The AMU was tasked to install and test needed software updates to the Graphical User Interface (GUI) and data acquisition prior to the February 2001 ABFM deployment. These updates corrected the problems noted during the June 2000 deployment such as interruptions in the data transmission and issues with starting and stopping the data acquisition.

Preparations for the February ABFM field experiment were completed by the end of January. Mr. Oram of SMG visited the AMU on 11 January to discuss the issues concerning ABFM support. Mr. Oram installed an updated version of the GUI software. This software converts SIGMET IRIS images to McIDAS files and overlays the aircraft position and altitude on the converted images in real time while tracking the ABFM aircraft. Also, Mr. Dianic updated and installed the pre-processing software that decodes, filters, and reformats aircraft position data prior to sending the data to the ABFM GUI display. A sample ABFM flight case was developed to test the downlink interfaces and aircraft track display.

Mr. Wheeler provided technical support during the ABFM field experiment in February. Very few data were collected and the field experiment was ended a week early as very little relevant weather occurred. All data for the February deployment were archived to tape and forwarded to Dr. Merceret. Another field experiment is planned for June 2001.

SUBTASK 13 MINISODAR™ EVALUATION (DR. SHORT AND MR. WHEELER)

The MiniSODAR™ (hereafter MinSO) is an acoustic wind profiler from AeroVironment, Inc., that provides vertical profiles of wind speed and direction with high temporal and spatial resolution. The MinSO in this evaluation is a model 4000 system, providing wind estimates from 15 to 200 m every 5 m. The system is configured to retrieve profiles at 1-minute intervals. Boeing plans to install a MinSO at the new SLC 37 as a substitute for a tall wind tower. It will be used to evaluate the launch pad winds for the new Evolved Expendable Launch Vehicle (EELV) during ground operations and to evaluate LCC during launch operations. In order to make critical GO/NO GO launch decisions, the 45 WS Launch Weather Officers (LWOs) and forecasters need to know the quality and reliability of MinSO data.

The AMU was tasked to perform an objective comparison between the SLC 37 MinSO wind observations and those from the closest tall (≥ 204 ft) wind towers. However, Boeing has delayed the purchase of a MinSO for the SLC 37 site. Therefore, the 45 WS requested that the AMU use data from the Range Standardization and Automation (RSA) MinSO located at the False Cape site. This MinSO is the same model to be purchased by Boeing and provides identical resolutions and range. The nearest tall wind towers to the False Cape site are sites 110, 313 and 6. The AMU began collection of data from these towers and the MinSO in October 2000. This report discusses the sensor locations, data structures, and concerns with the proposed tasking that the AMU has identified.

Sensor Locations

Figure 1 shows the locations of the acoustic wind profiler and wind towers, and a schematic representation of the heights at which data are taken. The MinSO is located at the False Cape site about 150 m from the ocean beach and within 50 m of the Samuel C. Phillips Parkway. Tower 110 is the closest tall tower to the False Cape site, located approximately 3.55 km to the south. It has wind sensors at 54, 162 and 204 ft above ground level, or 16.5, 49.4 and 62.2 meters. Tower 313 has wind sensors at 54, 162, 204, 295, 374 and 492 ft (16.5, 49.4, 62.2, 89.9, 120.1 and 150 m) allowing comparisons nearer the limit of the acoustic profiler's range. However, tower 313 is located 7.1 km WNW of the False Cape site. Tower 6 has wind sensors up to the 204 ft level and is located 10.2 km south in a topographic setting that is nearer to the ocean than the 313 and 110 sites.

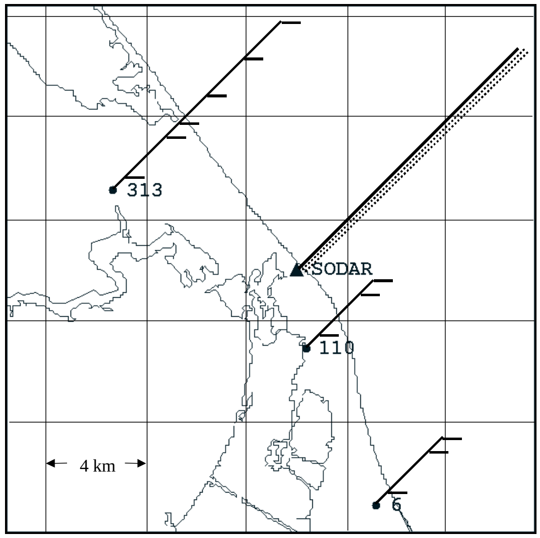

Figure 1. Locations of wind tower and MiniSODAR™ sensors used in a comparative study of wind speed, wind direction and data reliability. Tower height and sensor levels are indicated schematically. Towers 110 and 6 have sensors at 3 levels, up to a height of 204 ft. Tower 313 has sensors at 6 levels up to a height of 492 ft. The MiniSODAR™ has 38 levels of data at 5 m intervals from 15 to 200 m.

Data Structure

Figure 2 presents a time-height cross-section of the daily file structure of MinSO and wind tower data. The MinSO data is organized into hourly files with one-minute time resolution while the tower data is organized in six-hour files of one-minute data. Daily data files of each type were constructed by concatenating the hourly and six-hourly files and then monthly files were constructed by concatenating the daily files. Data from the acoustic wind profiler at heights of 15, 50, 60, 90, 120 and 150 m will be compared to wind tower data at the 54, 162, 204, 295, 374 and 492 ft levels.

Tasking Concerns

While collecting and analyzing the data, the AMU noted two issues that may hinder the results of the study. The first is the distance between the wind towers and the MinSO. The closest tall tower at site 110 is 3.55 km to the south and inland from the coast and the MinSO. The difference in terrain and the distance between the instruments may make the comparison between the two instruments problematic, as 1-minute turbulent variations in wind speed and direction are not coherent at such large distances. A comparison of longer-term averages may be affected by systematic differences in wind speed and direction between the near-shore environment and that farther inland. In addition, a comparison of longer-term averages may fail to properly characterize instrument characteristics on time scales of interest to operations. Towers 313 and 6 are even farther from the MinSO, and site 313 is farther inland than site 110. The second issue is that the MinSO has not been maintained by RSA since its installation; therefore the instrument may have calibration offsets or other problems that have not been attended to. The AMU will discuss these issues with the 45 WS and RSA personnel in April.

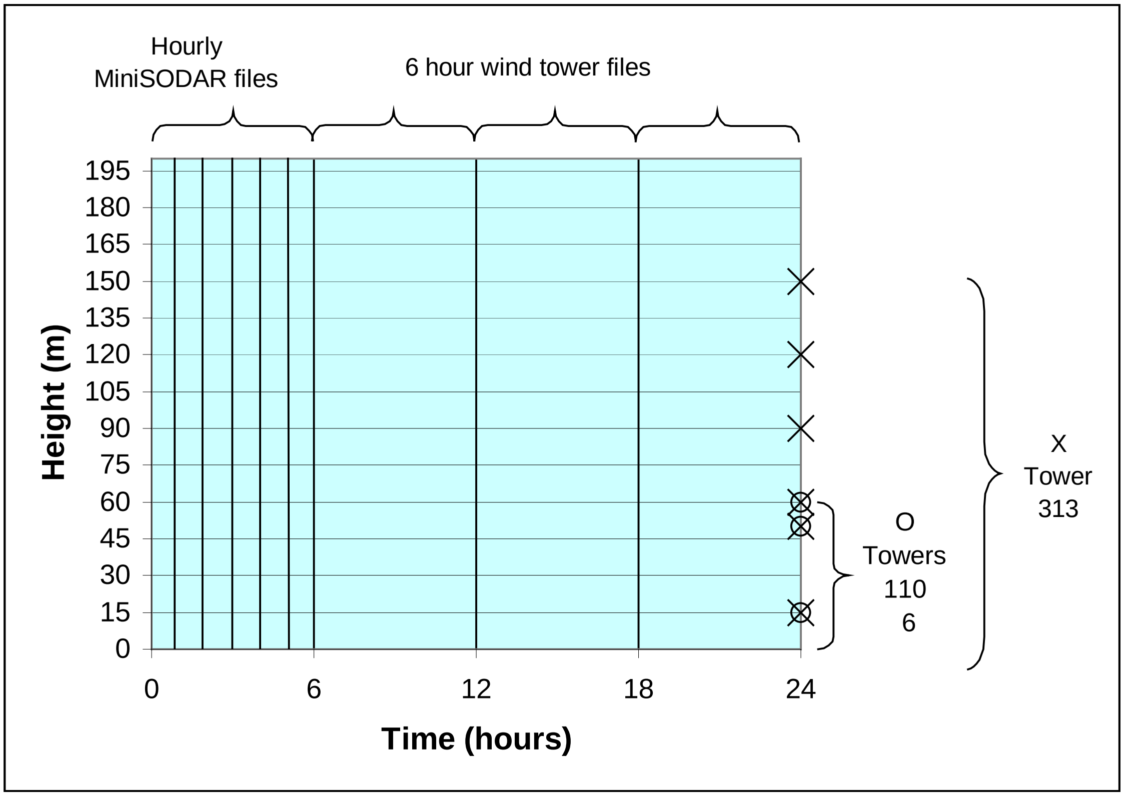

Figure 2. Time-height cross-section of the daily file structure of MiniSODAR™ and wind tower data. Heights of the tower sensor levels are indicated to the nearest 5 m. The acoustic profiler data has a vertical spacing of 5 m from 15 to 200 m.

SUBTASK 5 I&M AND RSA SUPPORT (DR. MANOBIANCO, MR. CASE, AND MR. WHEELER)

Dr. Manobianco and Mr. Case participated in a teleconference with Lt. Col. Dewey Harms (45 WS), Dr. Christy Crosier and Capt. Rick Gonzales (30th Weather Squadron; 30 WS), Brent Shaw (Forecast Systems Laboratory), and Mr. John Madura (NASA KSC Weather Office) regarding the choice of numerical weather prediction (NWP) model for the RSA program. Led by Lt. Col. Harms, the teleconference participants debated the advantages and disadvantages of running the Regional Atmospheric Modeling System (RAMS) versus the Pennsylvania State University-National Center for Atmospheric Research mesoscale model, version 5 (MM5) under the RSA program. The consensus at this teleconference was that MM5 is the preferred model for RSA due to several advantages of implementing MM5 instead of RAMS.

Mr. Wheeler reviewed slides and then participated in a teleconference with the 45 WS, KSC Weather Office, the 30 WS, Lockheed Martin (LM), and the Air Force on a LM proposal to change the RSA weather subsystems. The LM representatives proposed that the weather subsystem be migrated over to the NWS Advanced Weather Interactive Processing System (AWIPS), which would require several changes to the local area network configuration. Everyone was in favor, but final approval had not been given.

Table 5. AMU hours used in support of the I&M and RSA task in the second quarter of FY 2001 and total hours since July 1996.	
Quarterly Task Support (hours)	***Total Task Support (hours)***
4	311.5

2.3 TASK 005 MESOSCALE MODELING

SUBTASK 8 MESO-MODEL EVALUATION (MR. CASE)

The Eastern Range Dispersion Assessment System (ERDAS) is designed to provide emergency response guidance to the 45th Space Wing/Range Safety (45 SW/SE) in support of operations at the Eastern Range in the event of an accidental hazardous material release or an aborted vehicle launch. ERDAS uses the RAMS NWP model to generate prognostic wind and temperature fields for input into ERDAS diffusion algorithms. The RAMS model is run twice per day and generates 24-hour forecasts initialized at 0000 and 1200 UTC. In addition to winds and temperatures, RAMS predicts a number of other meteorological quantities on four nested grids with horizontal grid spacing of 60, 15, 5, and 1.25 km, respectively. Since the 1.25-km grid is centered over KSC/CCAFS, real-time RAMS forecasts provide an opportunity for improved weather forecasting in support of space operations through high-resolution NWP over the complex land-water interfaces of KSC/CCAFS. The 45 SW/SE and the 45 WS have tasked the AMU to evaluate the accuracy of RAMS for all seasons and under various weather regimes during 1999 and 2000.

During this past quarter, the draft of the ERDAS RAMS final report was completed and submitted for customer review. The final report contains a summary and description of an objective and subjective evaluation conducted for the 1999 Florida warm season (May to August), the 2000 warm season (May to September), and the 1999-2000 cool season (November to March). The objective evaluation consists of point error statistics for both the 1999-2000 cool and 2000 warm seasons at several observation locations, and point error statistics under various meteorological regimes for the 2000 warm-season. The subjective evaluation consists of a verification of the onset and propagation of the East Coast Sea Breeze (ECSB) for the 1999 and 2000 warm-seasons, and a precipitation and thunderstorm initiation verification experiment for the 2000 warm season.

The following sections will describe the classification of RAMS surface point forecast errors at the KSC/CCAFS wind towers during the 2000 Florida warm season, according to observed surface wind regimes. A description of the methodology is followed by the results of the surface wind-regime classification within the KSC/CCAFS wind-tower network.

Methodology for Surface Wind Regime Classification

The RAMS point forecast error statistics were calculated with regard to specific observed surface wind regimes as measured within the KSC/CCAFS wind-tower network. During each day, the surface wind regime was identified according to the early morning wind flow observed within the KSC/CCAFS wind towers. The days were then grouped into three classes of wind-flow patterns: westerly (offshore), easterly (onshore), and light, where light wind regimes were defined as sustained speeds less than 5 knots. The RAMS forecasts were grouped together according to the similar surface wind regimes and error statistics were compiled for the similar wind regimes.

The point forecast error statistics calculated under the three surface wind regimes include the root mean square (RMS) error, bias, and error standard deviation (SD) for temperatures and winds. By applying the Murphy (1988) decomposition for RMS error, the SD of the errors were estimated by

$$\mathrm{SD} = \sqrt{\mathrm{RMS}^2 - \mathrm{Bias}^2}\ .$$

RMS errors can be considered the total error or total difference between the RAMS forecasts and observations, whereas the bias represents the systematic error and the error SD is the non-systematic or random component of the error. In addition to error quantities, the average values of temperature forecasts and observations were computed as a function of forecast hour under each surface wind regime.

RAMS Errors under Specific Surface Wind Regimes

Table 6 summarizes the total number of days for the RAMS 0000 and 1200 UTC forecast cycles that were classified into the onshore (easterly), offshore (westerly), and light wind regimes. The forecasts that comprise each of these classifications were grouped together and point forecast error statistics at the KSC/CCAFS wind towers were calculated under each wind regime. The discussions for temperature, wind direction, and the individual wind component errors are given below only for the 1200 UTC forecast cycle.

Table 6. The number of days experiencing morning surface winds of onshore (easterly), offshore (westerly), and light or light and variable. Less than 5-kt wind speeds were classified as light.

RAMS Cycle	Onshore	Offshore	Light
0000 UTC	41	44	32
1200 UTC	46	49	35

Temperature Errors

The 1200 UTC forecast cycle temperature errors for each surface wind regime are shown in Figure 3. The westerly flow regime tends to yield higher predicted daytime temperatures in RAMS as evidenced by the mean temperature plots in Figure 3a. Among the three surface wind regimes, the light wind regime has the largest RMS error and cold bias during the afternoon and evening hours (6-12 hour forecasts in Figures 3b and c). The easterly and light wind regimes have a nearly identical pattern of random errors given by the SD in Figure 3d; however, the random portion of the westerly wind regime errors are substantially larger than the other two wind regimes during the late afternoon and evening hours. It is interesting to note that the smallest daytime bias occurs with the westerly wind regime as well.

This relatively larger random error during westerly surface winds is likely the result of an increased occurrence of convection in the vicinity of KSC/CCAFS under this flow regime. Depending on the strength, westerly low-level flow maintains the ECSB boundary in the vicinity of KSC/CCAFS, providing a focusing mechanism for afternoon and evening convection (López and Holle 1987). This convection can subsequently produce significant outflow boundaries resulting in localized temperature gradients and large random errors between the RAMS predicted and observed wind-tower temperatures.

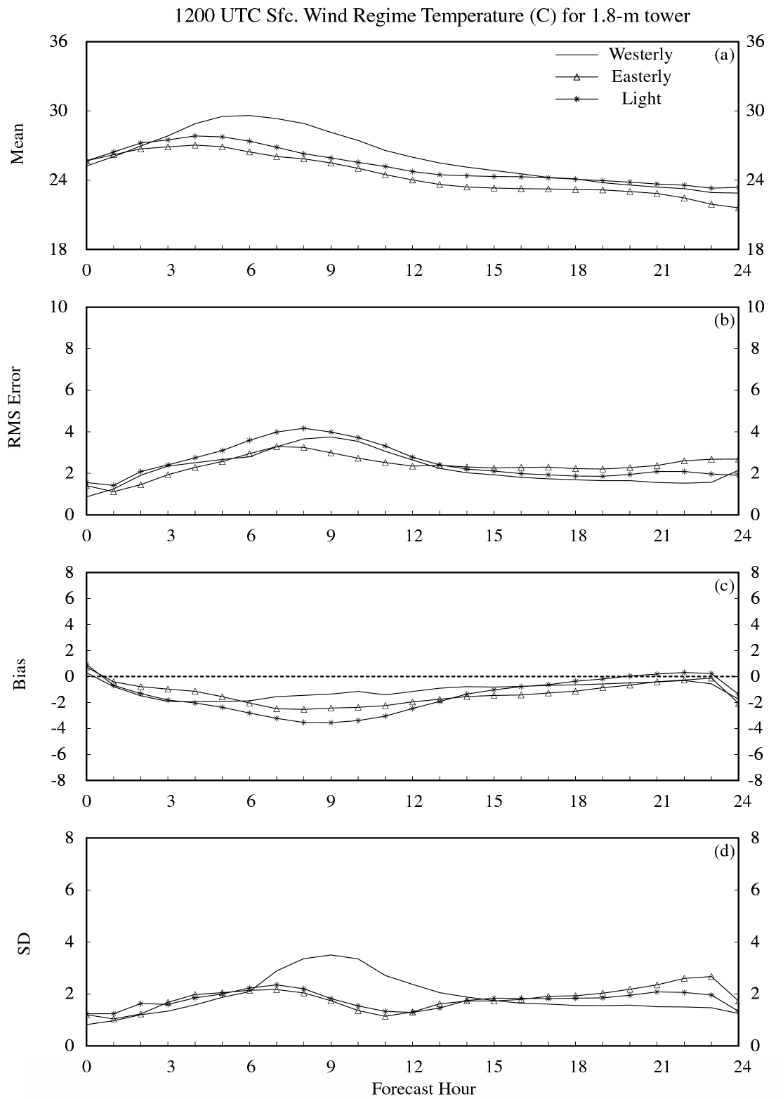

Figure 3. A meteogram plot of the 1200 UTC RAMS temperature errors (°C) during westerly (solid line), easterly (⊗), and light surface wind regimes (∗) for the 2000 Florida warm season. The temperature is verified at the 1.8-m level of the KSC/CCAFS wind-tower network. Parameters plotted as a function of forecast hour are a) mean forecast temperature under each wind regime, b) RMS error, c) bias, and d) error standard deviation.

Wind Direction

The results of the wind-regime classification reveal two apparent characteristics of the wind direction errors. First, the westerly wind regime contains the largest RMS error during the afternoon and evening hours, likely associated with the higher frequency of convection under low-level westerly flow. Second, the light wind regime is the primary contributor to the relatively large RMS errors during the late night and early morning hours, as anticipated. Under westerly wind flow, the 1200 UTC wind direction RMS errors reach a maximum of 70–80° between 9–11 hours (2100–2300 UTC, Figure 4a). Meanwhile, the RMS errors associated with easterly wind flows are quite small. In fact, during most of the afternoon and evening hours, the RMS error under easterly flow is under 30° (Figure 4a). Finally, the daytime RMS errors in light wind regimes fall between that of westerly and easterly wind flows.

The largest 1200 UTC wind direction errors are associated with the light winds that occur between 0–3 hours and 18–24 hours (Figure 4). The RMS error peaks at 90° at 21 hours (0900 UTC) whereas the bias drops to -30° at 21 and 22 hours. The RMS error grows substantially from 30–70° in the first two forecast hours of the light wind regime (Figure 4a) before tapering as mean wind speeds increase markedly during the day (not shown). These results illustrate how the variable nature of light winds leads to large errors in wind direction. The wind direction errors must be used with caution, though, because as wind speeds approach zero, the wind direction becomes an increasingly meaningless quantity. In these instances, an examination of the individual wind component errors is more appropriate to determine the representative magnitude of the wind errors.

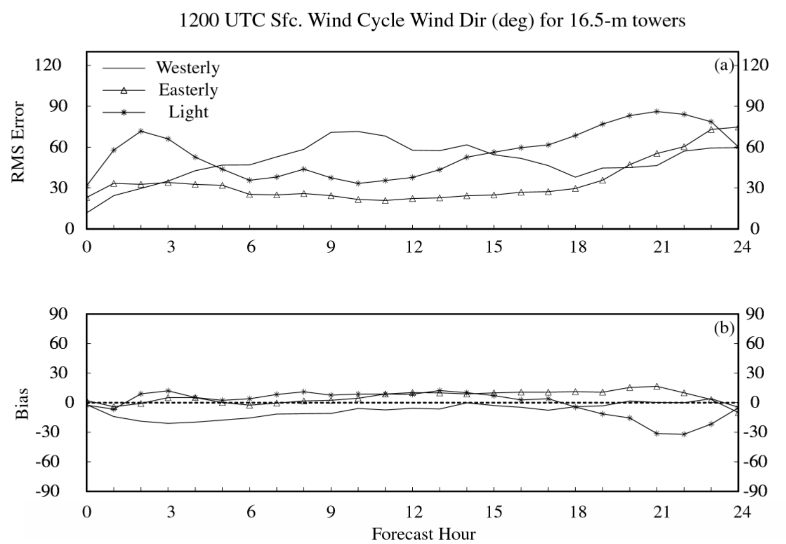

Figure 4. A meteogram plot of the 1200 UTC RAMS wind direction errors (deg.) during westerly (solid line), easterly (⊗), and light surface wind regimes (∗) for the 2000 Florida warm season. The wind direction is verified at the 16.5-m level of the KSC/CCAFS wind-tower network. Parameters plotted as a function of forecast hour are a) RMS error, and b) bias.

Wind Components

The distribution of mean forecast u-winds in the KSC/CCAFS wind tower network during the 1200 UTC cycle is shown in Figure 5. Based on this wind-flow classification, the mean forecast sea-breeze passage occurs at the latest time under westerly flow, given by the transition from positive (westerly) to negative (easterly) u winds. Under westerly wind flow, the mean forecast u-wind is between 0–2 m s^{-1} until 5 hours (1700 UTC), then becomes negative (easterly) with the mean passage of the sea breeze thereafter. In light regimes, the forecast u-wind is initially close to zero and then maintains an easterly component at all hours thereafter until 21hours (0900 UTC). Under easterly surface flow, the mean forecast u-wind generally remains less than -2 m s^{-1} at all hours. RAMS predicts the strongest post-sea breeze easterly flow under easterly wind regimes (Figure 5a).

While no dramatic variations are evident in the v-wind errors under different wind regimes (not shown), the u-wind errors show some interesting behavior. In the 1200 UTC cycle, the largest u-wind RMS errors (3–4 m s^{-1}) occur between 5–12 hours under westerly flow (Figure 5b). The easterly and light wind regimes have somewhat smaller errors during the afternoon and evening hours with similar magnitudes at about 2 m s^{-1}. All three regimes have comparable errors between 0–3 hours and 13–24 hours. The biases for each regime are generally similar and indicate that RAMS develops an easterly bias (negative u-wind bias) under all wind regimes during the afternoon and evening hours. Meanwhile, the error SD patterns closely follow that of the RMS errors, suggesting that much of the u-wind error under westerly wind flow is random in nature. The v-wind random errors are generally largest under westerly flow during the afternoon hours as well (not shown).

The relatively large random u-wind error during westerly flow could be the result of two factors. First, when surface winds are sufficiently strong from the west, the ECSB typically remains close to the east coast of Florida within the KSC/CCAFS wind-tower domain. If the RAMS model has just a small error in the location or timing of the ECSB then large random errors in the u-wind can result in the wind-tower network. Second, as mentioned previously, convection is most prevalent in east-central Florida under westerly flow since the focusing mechanism for convection (i.e. the ECSB) remains near KSC/CCAFS. Errors between observed and model-predicted convection can also lead to large random wind errors.

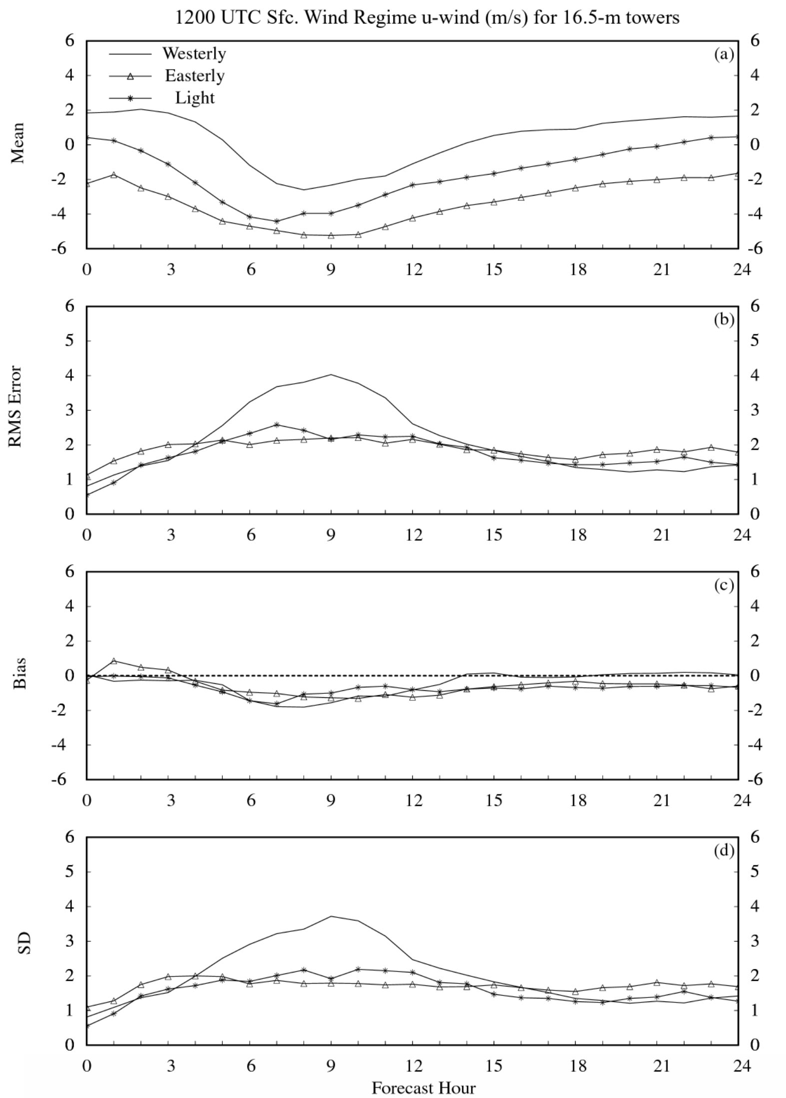

Figure 5. A meteogram plot of the 1200 UTC RAMS u-wind component errors (m s^{-1}) during westerly (solid line), easterly (⊗), and light surface wind regimes (∗) for the 2000 Florida warm season. The u-wind is verified at the 16.5-m level of the KSC/CCAFS wind-tower network. Parameters plotted as a function of forecast hour are a) mean forecast u-winds under each wind regime, b) RMS error, c) bias, and d) error standard deviation.

For more information, or to obtain a copy of the interim report, contact Mr. Jonathan Case by phone at 321-853-8264 or by email at case.jonathan@ensco.com.

References

López, R. E., and R. L. Holle, 1987: Distribution of summertime lightning as a function of low-level wind flow in central Florida. Technical Memorandum, NOAA Environmental Research Labs, Boulder, CO, 43 p.

Murphy, A. H., 1988: Skill scores based on the mean square error and their relationships to the correlation coefficient. *Mon. Wea. Rev.*, **116**, 2417-2424.

SUBTASK 10 LOCAL DATA INTEGRATION SYSTEM PHASE III (MR. CASE)

The Local Data Integration System (LDIS) task emerged out of the need to simplify the generation of short-term weather forecasts in support of launch, landing, and ground operations. The complexity of creating short-term forecasts has increased due to the variety and disparate characteristics of available weather observations. Therefore, the goal of the LDIS task is to generate high-resolution weather analysis products that may enhance the operational forecasters' understanding of the current state of the atmosphere, resulting in improved short-term forecasts. In Phase I, the AMU configured a prototype LDIS using the Advanced Regional Prediction System (ARPS) Data Analysis System (ADAS). The LDIS integrated all available weather observations into gridded analyses covering east-central Florida. In Phase II, the AMU simulated a real-time LDIS configuration using two weeks of archived data. The LDIS Phase III task calls for AMU assistance to SMG and NWS MLB to install a working real-time LDIS that routinely generates high-resolution products for operational guidance.

Radar Data Ingest at NWS Melbourne

Based on the lack of success with previous radar data ingest procedures, the AMU examined an alternative method for ingesting real-time Level II Weather Surveillance Radar 1988 Doppler (WSR-88D) data into the LDIS at NWS MLB. An ongoing effort titled the Collaborative Radar Acquisition and Field Test (CRAFT) involves saving Level II radar data to compressed files on a local workstation for distribution to participating organizations across the United States (refer to http://geosciences.ou.edu/~kkd/craft.htm). The AMU obtained the CRAFT compression and ingestion software from the University of Oklahoma and began building and configuring the software for the Hewlett Packard (HP) hardware platform as used at NWS MLB. Mr. Case traveled to NWS MLB in February to install and test the CRAFT data ingestion software. Unfortunately, the CRAFT software was not able to read and ingest the Level II WSR-88D data in real-time on the HP workstation. As with previous software from the National Severe Storms Laboratory (NSSL), the CRAFT software is not supported or tested on an HP hardware platform.

Based on the lack of success in installing and configuring real-time radar ingest software on the HP platform, the NWS MLB decided to configure an available Sun workstation for the radar data ingestion. In addition, the LDIS can be eventually configured to run in real-time on the Sun platform since the ADAS from the University of Oklahoma is tested and supported for Sun hardware. By early April, the level II WSR-88D data ingestion was configured and ran properly on the NWS MLB Sun workstation. Finally, Mr. Case successfully installed the Level II radar-remapping program that maps the WSR-88D reflectivity and radial velocity data to the analysis grid, allowing radar data ingest into the LDIS every 15 minutes.

LDIS Phase III Memorandum

The AMU finalized and distributed a memorandum describing the issues involved with installing and configuring a real-time version of LDIS at the SMG and NWS MLB offices. This memorandum was designed to formally document the transition of LDIS to real time and to offer a guideline for other forecast offices interested in running an LDIS.

SUBTASK 11 EXTENSION / ENHANCEMENT OF THE ERDAS RAMS EVALUATION (MR. CASE AND MR. DIANIC)

The Extension / Enhancement of the ERDAS RAMS Evaluation is being funded by KSC under AMU option hours. During the course of the evaluation under Subtask 8 (Meso-Model Evaluation), the AMU discovered a systematic low-level cold bias in the RAMS forecasts. In addition, several RAMS forecasts were not successfully run in real-time due to various technical issues. As a result, KSC tasked the AMU to re-run historical RAMS forecasts to improve the archived data base, and to perform sensitivity tests to identify the possible cause(s) for the model cold bias. Also, depending on the remaining funds in the options hours task, the AMU will explore the possibility of transferring real-time RAMS forecasts to the NWS MLB and SMG offices, and to improve the ENSCO-generated graphical user interface that verifies RAMS forecasts in real time.

During this past quarter, the AMU prepared a draft memorandum that discusses a proposed data transfer mechanism for sending a small subset of real-time RAMS forecasts to SMG and NWS MLB. The memorandum also examines the issues and difficulties encountered during the testing phase of this data transfer technique. The memorandum continues to undergo customer review due to several issues raised by AMU customers.

The AMU also completed the recovery of RAMS 3-grid forecasts for the 1999-2000 cool season that were lost due to a disk crash. The AMU generated RAMS 3-grid forecasts by withholding the innermost grid (grid 4) during model integration while keeping all the other settings the same. This sensitivity experiment was conducted to determine the impact of a coarser resolution inner grid on the subsequent objective point error statistics during the 1999-2000 cool season. Once the RAMS forecasts were fully recovered, the AMU processed the error statistics for the RAMS 4-grid/3-grid comparison experiment for the 1999-2000 cool-season.

Finally, a variety of scripts were completed to run RAMS sensitivity experiments on the AMU HP workstation. A few RAMS sensitivity forecasts were performed to try to isolate the cause(s) of some of the errors in the RAMS model, particularly the low-level cold bias. Based on these sensitivity experiments, it appears that the development of a persistent, widespread fog deck near the surface is the cause of the daytime low-level cold temperature bias in RAMS. However, the physical mechanism causing this anomalous low-level fog deck was not identified.

2.4 AMU CHIEF'S TECHNICAL ACTIVITIES (DR. MERCERET)

Dr. Merceret participated in and managed the February field campaign of the Lightning Launch Commit Criteria program (also known as ABFM). He submitted a study of the effect of temporal averaging on vertical spectra of horizontal wind components computed from wind profilers to the "Journal of Atmospheric and Oceanic Technology". He also participated in a software design workshop for the HyperSODAR. The HyperSODAR is a proprietary form of acoustic wind profiler developed under a NASA SBIR by Sensor Technology Research, Inc. Finally, Dr. Merceret led a technical discussion and tour of the KSC 50-MHz Doppler Radar Wind Profiler (DRWP) for the Titan Day of Launch Working Group #24. He also briefed the KSC Center Director and senior KSC officials on the use of the 50-MHz DRWP by Shuttle on the day of launch.

2.5 TASK 001 AMU OPERATIONS

The AMU Mid-Course Review teleconference was held on 29 March with representatives from the AMU, 45 WS, SMG, NWS MLB, and Marshall Space Flight Center (MSFC). A consensus was reached quickly on extending the RSA support and Local Data Integration System tasks, and on adding the Land-Breeze Forecasting task to the AMU schedule.

Mr. Wheeler developed the AMU's Information Technology (IT) Purchase Plan that identifies the planned and existing IT procurements for the current fiscal year. He developed the equipment and software requirements, researched possible solutions to those requirements, and received quotes for the procurements. Purchase requests (PRs) for new equipment and services for the AMU were submitted to NASA. By being submitted before the end of January 2001, one PR for a Linux Beowulf 32-processor cluster system saved NASA $15,000.

NOTICE

List of Acronyms

30 SW	30th Space Wing
30 WS	30th Weather Squadron
45 LG	45th Logistics Group
45 OG	45th Operations Group
45 SW	45th Space Wing
45 SW/SE	45th Space Wing/Range Safety
45 WS	45th Weather Squadron
ABFM	Airborne Field Mill
ADAS	ARPS Data Analysis System
AFIT	Air Force Institute of Technology
AFRL	Air Force Research Laboratory
AFSPC	Air Force Space Command
AFWA	Air Force Weather Agency
AMU	Applied Meteorology Unit
ARPS	Advanced Regional Prediction System
AWIPS	Advanced Weather Interactive Processing System
CCAFS	Cape Canaveral Air Force Station
CRAFT	Collaborative Radar Acquisition and Field Test
CSR	Computer Sciences Raytheon
DRWP	Doppler Radar Wind Profiler
ECSB	East Coast Sea Breeze
EELV	Evolved Expendable Launch Vehicle
EOM	End of Mission
ERDAS	Eastern Range Dispersion Assessment System
FAR	False Alarm Rate
FR	Shuttle Flight Rules
FSL	Forecast Systems Laboratory
FSU	Florida State University
FY	Fiscal Year
GUI	Graphical User Interface
HP	Hewlett Packard
IRIS	SIGMET's Integrated Radar Information System
IUW	IRIS User's Workshop
IT	Information Technology
JSC	Johnson Space Center
KSC	Kennedy Space Center
LCC	Launch Commit Criteria
LDIS	Local Data Integration System
LM	Lockheed Martin
LWO	Launch Weather Officer
McIDAS	Man-computer Interactive Data Access System

List of Acronyms

MIDDS	Meteorological Interactive Data Display System
MM5	Penn State/NCAR Mesoscale Model version 5
MSFC	Marshall Space Flight Center
MinSO	MiniSODAR™
NASA	National Aeronautics and Space Administration
NCAR	National Center for Atmospheric Research
NOAA	National Oceanic and Atmospheric Administration
NSSL	National Severe Storms Laboratory
NWP	Numerical Weather Prediction
NWS MLB	National Weather Service in Melbourne, FL
NPTPI	Neumann-Pfeffer Index
OBS	Observations-Based equations
PCLIMO	Persistence Climatology equations
POD	Probability of Detection
RAMS	Regional Atmospheric Modeling System
RFQ	Request for Quotation
RMS	Root Mean Square
RSA	Range Standardization and Automation
RTLS	Return to Launch Site
SLC	Space Launch Complex
SD	Standard Deviation
SLF	Shuttle Landing Facility
SLTI	Stratified Logistic Thunderstorm Index
SMC	Space and Missile Center
SMG	Spaceflight Meteorology Group
SRH	NWS Southern Region Headquarters
UPI	User Product Insert
USAF	United States Air Force
UTC	Universal Coordinated Time
WSR-74C	Weather Surveillance Radar, model 74C
WSR-88D	Weather Surveillance Radar 1988 Doppler
WWW	World Wide Web

Appendix A

AMU Project Schedule 30 April 2001				
AMU Projects	**Milestones**	**Scheduled Begin Date**	**Scheduled End Date**	**Notes/Status**
Statistical Forecast Guidance (Ceilings)	Determine Predictand(s)	Aug 98	Sep 98	Completed
	Data Collection, Formulation and Method Selection	Sep 98	Apr 99	Completed
	Equation Development, Tests with Independent Data, and Tests with Individual Cases	Apr 00	Dec 00	Completed
	Prepare Products, Final Report for Distribution	Jan 00	Apr 01	Behind Schedule – Task lead on extended leave due to family emergency
Statistical Forecast Guidance (Winds)	Determine Predictand(s)	Mar 01	Apr 01	Behind Schedule – Waiting to complete ceiling stats task
	Data Reduction, Formulation and Method Selection	Apr 01	May 01	Behind Schedule – Waiting to complete ceiling stats task
	Equation Development, Tests with Independent Data, and Tests with Individual Cases	May 01	Sep 01	On Schedule
	Prepare Products, Final Report for Distribution	Sep 01	Dec 01	On Schedule
Meso-Model Evaluation	Develop ERDAS/RAMS Evaluation Protocol	Feb 99	Mar 99	Completed
	Perform ERDAS/RAMS Evaluation	Apr 99	Sep 99	Completed
	Extend ERDAS/RAMS Evaluation	Oct 99	Nov 00	Completed
	Interim ERDAS/RAMS Report	Dec 99	Aug 00	Completed
	Final ERDAS/RAMS Report	Oct 00	Apr 01	Undergoing internal review
SIGMET IRIS Processor Evaluation Phase II	Develop and transition new products to 45 WS IRIS station	Apr 00	Apr 01	Rescheduled – Customer to re-scope task based on AMU preliminary results
	Final Report	May 01	Jun 01	On Schedule

AMU Project Schedule 30 April 2001				
AMU Projects	Milestones	Scheduled Begin Date	Scheduled End Date	Notes/Status
LDIS Extension: Phase III	Assistance in installation at NWS MLB	Jan 00	Jan 01	Completed – Except for radar data ingestor at NWS MLB
	Assistance in installation at SMG	Apr 00	Jul 00	Completed
	Memorandum describing LDIS transition to real-time operations	Jul 00	Feb 01	Completed
	Technical collaboration with SMG towards a conference paper	Aug 00	May 01	Conference papers will be submitted by 1 May
ERDAS RAMS Extension Task	Memorandum summarizing data transfer feasibility to SMG & NWS MLB	Jul 00	Apr 01	Undergoing external review
	Enhancement of verification Graphical User Interface	Apr 00	Apr 01	Behind Schedule– Data recovery took longer than expected
	Develop data transfer	Sep 00	Mar 01	Completed
	Input of methodology and results into ERDAS RAMS final report	Nov 00	Mar 01	Completed
MiniSODAR Evaluation	Collection and processing of data	Oct 00	Sep 01	On Schedule
	Analysis and objective comparison	Jan 01	Oct 01	On Schedule
	Final Report	Oct 01	Apr 02	On Schedule
Neumann-Pfeffer TSTM Probability Index	Convert Software	Oct 01	Jan 01	Completed
	Write data decoders, transition to RWO PC, and prepare documentation	Jan 01	Jun 01	On Schedule